Engineering Innovations
ISSN: 2813-1002, Vol. 15, pp 1-8
doi:10.4028/p-V4p5sx
© 2025 The Author(s). Published by Trans Tech Publications Ltd, Switzerland.
Submitted: 2025-07-21
Revised: 2025-10-06
Accepted: 2025-10-06
Online: 2025-11-18

Analysis of the Dislocation Structure, Kinetics and Dynamics in the High-Entropy Alloy $Al_{0.5}CoCrCuFeNi$

VASILIJ Natsik[1,a*], YURI Semerenko[1,b], NIKOLAI Galtsov[1,c], DIANA Hurova[1,d], VICTOR Zoryansky[1,e], ELENA Tabachnikova[1,f], TAMARA Bednarchuk[2,g], PETER Zinoviev[1,h]

[1]B. Verkin Institute for Low Temperature Physics and Engineering of the National Academy of Sciences of Ukraine, 47 Nauky Ave., 61103 Kharkiv, Ukraine

[2]Institute of Low Temperature and Structure Research, Polish Academy of Sciences, P.O. Box 1410, 50-950 Wroclaw, Poland

[a]natsik@ilt.kharkov.ua, [b]semerenko@ilt.kharkov.ua, [c]galtsov@ilt.kharkov.ua, [d]hurova@ilt.kharkov.ua, [e]zoryansky@ilt.kharkov.ua, [f]tabachnikova@ilt.kharkov.ua, [g]t.bednarchuk@intibs.pl, [h]zinoviev@ilt.kharkov.ua

Keywords: high entropy alloy; acoustic relaxation; plastic deformation, X-ray structural analysis, dislocation model

Abstract. A theoretical analysis of low-temperature plastic deformation processes and acoustic relaxation in the high-entropy alloy $Al_{0.5}CoCrCuFeNi$ has been conducted. Within the framework of proposed dislocation model it was established the key types of dislocation defects in the alloy's lattice structure; types of barriers that hinder the movement of dislocation lines (strings); and mechanisms of thermally activated movement of various dislocation line elements through these barriers at room and low temperatures. Using this model, quantitative estimates have been derived for significant dislocation characteristics and their interaction with barriers, such as the distance between local obstacles in the slip plane ~ 4 nm, the Peierls stress for dislocations in an easy slip system $4 \cdot 10^6$ Pa, and more. Additionally, an estimated speed of sound $3.4 \cdot 10^3 \frac{m}{s}$ based on the proposed model aligns well with the direct experimental data. The empirical estimates for the energy per unit length of a dislocation $\sim 10^{-8} \frac{J}{m}$ and the linear mass density $\sim 10^{-15} \frac{\text{kg}}{m}$ are consistent with modern continuum dislocation theory. A detailed examination of the structure of the alloy $Al_{0.5}CoCrCuFeNi$ was carried out using X-ray diffraction and Energy Dispersive Spectroscopy techniques. Numerical estimates of the dislocation density $\sim 5 \cdot 10^{15} m^{-2}$ were obtained through Williamson–Hall analysis of X-ray diffraction patterns. It was found to correlate with the estimates overall length of dislocation segments per unit volume which effectively interacts with elastic vibrations of the sample $\sim 4 \cdot 10^{13} m^{-2}$, as determined from acoustic relaxation measurements.

Introduction

High-Entropy Alloys (HEAs) are metallic systems consisting of five or more elements with nearly equiatomic concentrations. These alloys exhibit enhanced mixing entropy and possess an advantageous balance of strength and ductility, along with exceptional resistance to thermal and mechanical effects.

One of the representative HEAs with an fcc lattice is $Al_{0.5}CoCrCuFeNi$ [1]. Its mechanical and acoustic properties at temperatures below 300 K have been studied in detail in [1], [5]-[9]. In this paper, we consider the relationship between the properties analyzed in [5]-[8]. We consider the application of the fundamental principles of modern dislocation theory to interpret these properties. Our study uses data from X-ray structural analysis, resonance mechanical spectroscopy [8], and the active deformation method [7].

This article is an open access article under the terms and conditions of the Creative Commons Attribution (CC BY) license (https://creativecommons.org/licenses/by/4.0)

Studied Samples

The ingot of the multicomponent high-entropy alloy $Al_{0.5}CoCrCuFeNi$ was obtained by remelting high-purity ≈ 99.9% elements on a copper hearth with water cooling in an arc furnace, using a non-consumable tungsten electrode in a purified argon atmosphere. To ensure a uniform distribution of elements, the ingot was subjected to five remelting cycles, periodically flipped on the hearth.
The electron microscopy imaging of the sample and its elemental composition were studied using Field Emission Scanning Electron Microscope (FE-SEM) FEI Nova NanoSEM 230 (FEI Company, Hillsboro, USA) along with energy dispersive X-ray spectrometer EDAX Genesis XM4 (EDAX Inc., Mahwah, USA). Fig. 1 shows the results of determining the averaged elemental composition of the alloy under study.

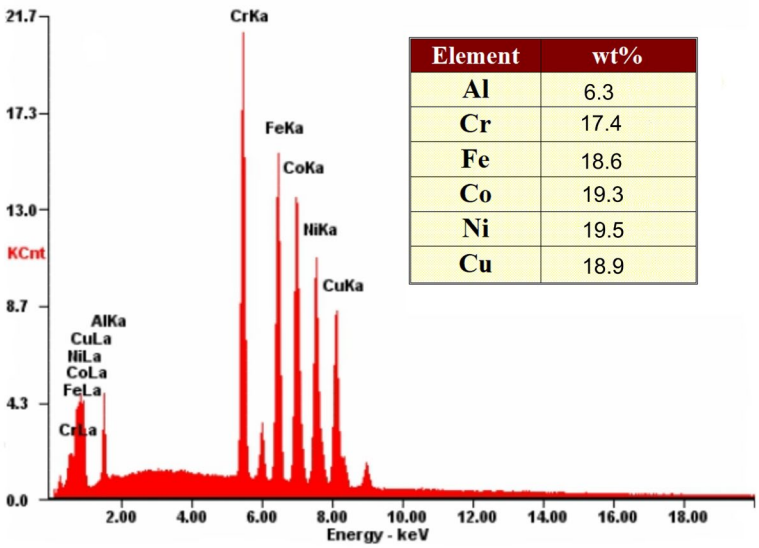

Element	wt%
Al	6.3
Cr	17.4
Fe	18.6
Co	19.3
Ni	19.5
Cu	18.9

Fig. 1 The EDS patterns for the high-entropy alloy $Al_{0.5}CoCrCuFeNi$ in state (**II**). The transition from structural state (**I**) to state (**II**) (annealing of the sample) does not change its chemical composition as a whole.

The metallographic analysis [6] reveals that the microstructure of the alloy exhibits a characteristic dendritic pattern, consisting primarily of a dense body of dendrites as the main structural component, along with interdendritic spaces. Data of scanning electron microscopy using an X-ray microanalyser show that the elemental composition of dendrites and interdendritic spaces is significantly different [6].

The alloy was examined in two structural states: (**I**) the as-cast coarse-grained state and (**II**) after high-temperature annealing in vacuum at 1250 K for 6 hours. After annealing, the samples were cooled together with the furnace (the cooling rate to 770 K was 5 degrees/min). It was established that annealing leads to a significant change in the alloy structure and the chemical composition of the structural regions [6], but does not change the chemical composition of the sample as a whole.

Dislocation Structure

The X-ray diffraction (XRD) patterns of the high-entropy $Al_{0.5}CoCrCuFeNi$ alloy ingot were studied in state (**II**). XRD measurements were carried out using a PANalytical X'pert Pro diffractometer (PANalytical B.V., Almelo, Netherlands) at the Institute of Low Temperatures and Structural Research of the Polish Academy of Sciences. XRD patterns were recorded at room temperature in Bragg-Brentano geometry over 2θ range: from 30° to 120°, with a Cu-K_α anode radiation. Numerical estimates of the average value of dislocation density $\bar{\rho} \simeq 5 \cdot 10^{15} m^{-2}$ and the average value of coherent scattering regions size $\bar{D} \simeq 18\, nm$ were obtained through Williamson–Hall analysis [10] of XRD patterns (Fig. 2). Such a small value of $\bar{D}$ in a coarse-grained annealed sample may indicate the presence of a large number of low-angle boundaries.

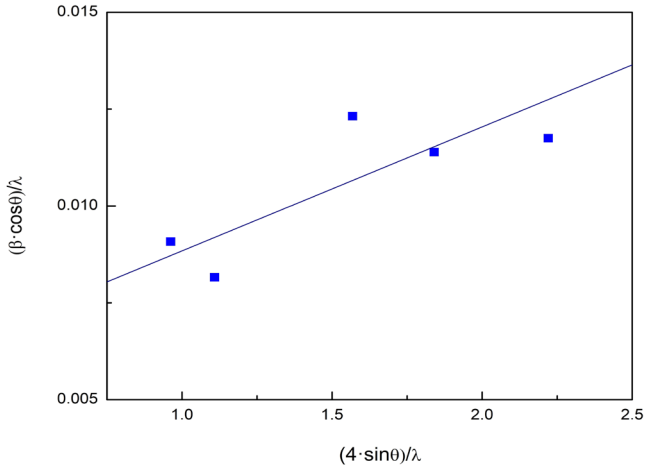

Fig. 2 Williamson–Hall plot for the specimens of the high-entropy alloy $Al_{0.5}CoCrCuFeNi$ in state (**II**). λ is the X-ray wavelength; β is a instrument-corrected physical value of the Full Width at Half Maximum (FWHM) of Bragg peak.

Acoustic properties

The temperature dependence of internal friction $Q_{exp}^{-1(T)}$ and dynamic Young's modulus $E(T)_{exp}$ was investigated in [8] using the mechanical resonance spectroscopy method. The approach for these experiments was detailed in [11]. For state (**I**) the temperature dependencies $Q_{exp}^{-1(T)}$ and $E(T)_{exp}$ do not exhibit any notable features, such as relaxation resonances. However, the transition to state (**II**) results in the emergence of the acoustic absorption peak (Fig. 3).

It has been established that the dependence $E(T)_{exp}$recorded in experiments can be divided into resonant $E_R(T)$ and background $E_0\beta T \cdot exp\left(-\frac{\Theta_E}{T}\right)$ components:

$$E(T)_0\left[1-\beta T\cdot exp\left(-\frac{\Theta_E}{T}\right)\right]_R(T)_{exp}, \quad (1)$$

here $E_0 \simeq 240$ GPa is the limit value of the module at $T \to 0$; coefficient $\beta \simeq 4\cdot 10^{-4}$ K^{-1} depends on the material and the vibration mode under study; Θ_E is the Einstein temperature of the material under study. This relation allowed us to obtain an estimate $\Theta_E = 160$ K for the Einstein temperature.

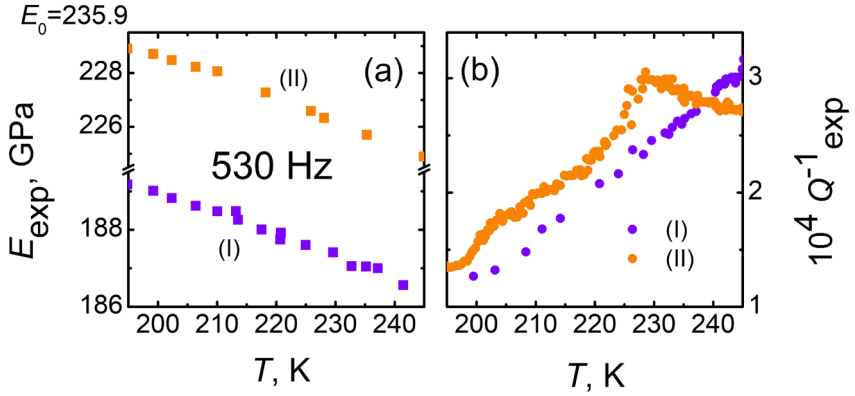

Fig. 3. Temperature dependences of the acoustic characteristics of the $Al_{0.5}CoCrCuFeNi$ alloy for two structural states [8]: a) temperature dependence of dynamic Young's modulus $E(T)_{exp}$, ■ – state (**I**), ■ – state (**II**); b) temperature dependence of internal friction $Q_{exp}^{-1(T)}$, ● – state (**I**), ● - state (**II**).

In previous works [8], [1] we came to the conclusion that the peak at $T_p \simeq 230$ K corresponds to the thermally activated separation of dislocation segments from point defects. The obtained values of activation energy $U_0 \simeq 0.4$ eV, effective oscillation period $\theta_0 \simeq 10^{-13}$ s and $C_r\Delta_0 \simeq 4 \cdot 10^{-4}$ (Δ_0 is the effective specific contribution of an individual relaxer with concentration C_r) are typical for Koiwa-Hasiguti relaxers in fcc metals. For Koiwa-Hasiguti relaxers $C_r\Delta_0 \sim 10^{-1}\rho_L L^3$ (L is the length of dislocation segments with volume density ρ_L which breaking away from an individual point defect) [12]. By making assumption $C_r \approx \rho_L$, we derive an estimate $\Delta_0 \sim 10^{-1}L^3$ for the contribution of one relaxer to internal friction and decreasing of the elastic modulus. Let us consider that small atomic clusters, spaced approximately a few nanometers apart, serve as local pinning centres for dislocation segments: they are recorded in state (**II**) by electron microscopy methods [4]. Then, when estimating the length L, we can take the twice distance between clusters $L \simeq 10 \div 20$ nm. This value is consistent with our estimate for coherent scattering regions size $\bar{D} \simeq 18\,nm$ and corresponds to the volume density of relaxers $C_r = \rho_L \sim 4 \cdot 10^{21}$ m^{-3}.

The dislocation density $\Lambda_d = L\rho_L$ (overall length of dislocation segments per unit volume, which effectively interact with elastic vibrations of the sample) yields the following estimate $\Lambda_d \sim 4 \cdot 10^{13}$ m^{-2}.

It was also established that the resonant component of acoustic relaxation in state (**II**) $Q_R^{-1}(T)$ contains both the main relaxation resonance (peak at $T_p \simeq 230$ K) and its satellite at $T_p^s = 190$ K, localized on the left slope of the main peak. Outlined in [8] statistical and thermal activation analysis leads us to the conclusion that the peak $T_{ps} = 190$ K is due to Seeger relaxation with parameters: $U_0^s \simeq 0.1$ eV, $\theta_0^s \simeq 4 \cdot 10^{-11}$ s, $C_r^s\Delta_0^s \simeq 10^{-4}$.

The motion equation for a dislocation string with linear mass density M in a sinusoidal first-kind Peierls relief admits soliton solutions in the form of kinks with the width $\lambda_k = \left(\frac{2\Gamma \cdot a_p}{\pi b \tau_{p1}}\right)^{0.5}$, mass $m_k = M \cdot \left(\frac{8ba_p^3\tau_{p1}}{\pi^3\Gamma}\right)^{0.5}$ and energy $\varepsilon_k = m_k c_t^2$; their properties was determined by the parameters of the potential and dislocation (here Γ represents the energy per unit length of a dislocation within the continuum approximation, also known as linear tension; $\frac{ba_p}{\pi}\tau_{p1}$ is the magnitude of barriers and τ_{p1} is the critical stress for the first-kind Peierls relief). The period of natural oscillations of a rectilinear segment in the relief valley is $\theta_{p1} = \pi \cdot \frac{\lambda_k}{c_t}$ and $c_t = \left(\frac{\Gamma}{M}\right)^{0.5}$ is the characteristic value of the speed of transverse sound vibrations in the crystal.

The average time $\theta(T)$ of thermally activated nucleation of kink–antikink pairs on a straight segment of a dislocation line is described by the Arrhenius law $\theta(T) = \theta_0^s \cdot exp\left(\frac{U}{k_B T}\right)$ (k_B is the Boltzman's constant) with activation energy $U = U_0^s \simeq 2 \cdot \varepsilon_k$ and attempt period $\theta_0^s \simeq \theta_{p1}$. The interaction of elastic vibrations $\tau \ll \tau_{p1}$ (τ - shear stress component in the slip plane) with such a process is one of the mechanisms of relaxation resonance [13]. It was established [1] that the discussed resonance $T_p^s = 190$ K in the studied HEA is caused by the Seeger process, therefore $C_r^s\Delta_0^s \approx 10^{-1}L^3\rho_L$ [14].

The parameters required for further evaluation of the studied HEA are as follows: Burgers vector $b = a_0 \simeq 3 \cdot 10^{-10}\,m$, period of Peierls relief in the direction of easy sliding $a_p = \frac{\sqrt{3}}{2} \cdot a_0 \approx 2 \cdot 10^{-10}\,m$ [7]; density $\rho \simeq 8 \cdot 10^3\ \frac{\text{kg}}{m^3}$ [6], shear modulus $G = \frac{1}{2} \cdot \frac{E}{1+\nu} \simeq 10^{11}$ Pa, Poisson's ratio $\nu \approx 0.2$ [2]. It leads to the following estimates: $\rho_L L^3 \leq 10^{-3}$, $M \simeq 10^{-15}\ \frac{\text{kg}}{m} \approx 2 \cdot \rho b^2$, $\Gamma \approx 13 \cdot 10^{-9}\ \frac{J}{m} \approx 2 \cdot Gb^2$.

The kink mass $m_k \approx 5 \cdot 10^{-3} m_a \approx 5 \cdot 10^{-28}$ kg can be compared to the average atomic mass m_a of the alloy under study, its width $\lambda_k \approx 40 \cdot a_0 \simeq 10^{-8}\,m$ to the minimum interatomic spacing a_0, and the Peierls critical stress $\tau_{p1} \approx 4 \cdot 10^6$ Pa $\approx 4 \cdot 10^{-5} G$ to the shear modulus G.

The obtained estimate $c_t = \left(\frac{G}{\rho}\right)^{0.5} \approx 3.4 \cdot 10^3 \ \frac{m}{s}$ aligns well with the available direct experimental data [2], [3].

Mechanical Properties

Mechanical testing of the alloy was conducted across a broad temperature range from 0.5 K to 300 K. The methodology for analyzing mechanical properties using the active deformation technique at a constant rate is outlined in [7]. The experimental results for both structural states (**I**) and (**II**) are shown in Fig. 4 at a given strain rate $\dot{\varepsilon} = 4 \cdot 10^{-4}$ s^{-1}. The work [1] shows that stage of linear strain hardening occurs at deformation $\varepsilon \approx 2\%$, therefore for this alloy stress $\tau_2(T) = \tau(\varepsilon = 2\%; T)$ should be considered as the yield stress. Previous studies have shown that the plastic deformation of the alloy under investigation is governed by the conservative motion of complete dislocations within the typical for fcc crystals slip system $\{111\}\langle 110\rangle$ [9]. The experimentally observed strong temperature dependence of $\tau_2(T)$ suggests that plastic deformation is thermally activated, with both Peierls barriers and local barriers potentially acting as controlling factors in dislocation movement. In the first case, the fundamental mechanism of plastic deformation involves the thermally activated nucleation of a paired kink on a dislocation segment within the Peierls relief, while in the second case, it consists of the thermally activated overcoming of a local barrier by a dislocation segment.

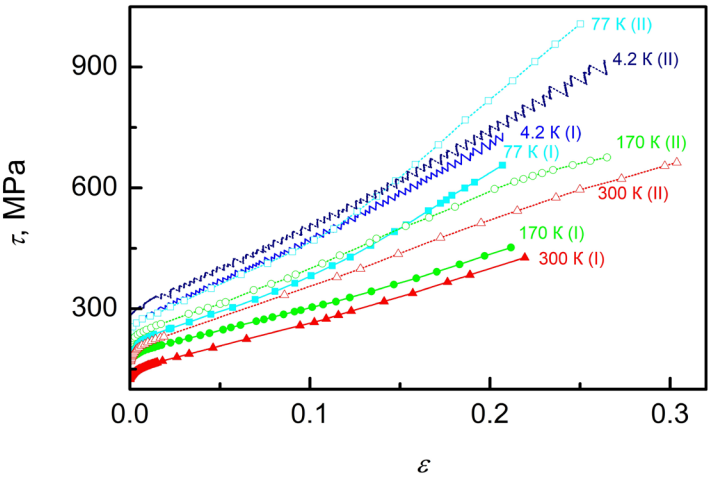

Fig. 4. Diagrams of compression deformation of the alloy $Al_{0.5}CoCrCuFeNi$ for two structural states (**I**) and (**II**) in $\tau - \varepsilon$ coordinates at different deformation temperatures [1].

Through the analysis of low-temperature acoustic resonances in the studied HEA, it was determined that in it the Peierls stress $\tau_{p1} \approx 4 \cdot 10^6$ Pa for dislocations in the easy slip system is significantly less than the low-temperature values of the yield strength $\tau_2 \approx 2 \cdot 10^8$ Pa $\approx 50 \cdot \tau_{p1}$. As a result, the Peierls relief has no substantial impact on the kinetics of low-temperature plastic deformation of this material; rather, it is governed by a sufficiently high volume density of local barriers.

Clusters of atoms from one of the alloy's constituent elements can serve as structural inhomogeneities that influence thermally activated plastic deformation in HEAs. Several neighbouring atoms of an element with a relatively large atomic radius generate local distortions in the crystal lattice, posing a considerable barrier to dislocation movement. Experimental observations in [4] have identified such clusters, with characteristic distances between them measuring several nanometers, i.e. for them $\simeq 10$ nm. These estimates also practically coincide with the estimates we obtained for the size of coherent scattering regions $\bar{D} \simeq 18\ nm$ and the twice distance between clusters $L \simeq 10 \div 20$ nm.

Thermal activation analysis [15] of experimental results make it possible to obtain estimates for the parameters of local barriers and the distances between them in slip planes: density of local obstacles controlling the movement of dislocations $S_0 = 260 \cdot b^2, \text{m}^2$, which corresponds to the distance between local obstacles in the sliding plane $l = (S_0)^{0.5} \simeq 16 \cdot b \simeq 4$ nm and the length of straight lines segments of dislocation lines located in the valleys of first kind Peierls relief $L = 2l \simeq 10$ nm. This value is in good agreement with the estimates obtained from the study of acoustic properties and X-ray structural studies.

Conclusion

A deep physical analysis of the mechanical, acoustic and structural properties of the alloy was performed. Quantitative estimates of various parameters of the proposed model were obtained, consistent with the experimental data of other authors. Thus, the proposed dislocation model does not simply describe the behavior of dislocations in the material under study, but links acoustic properties, thermodynamics and microstructure into a single picture.

- It is shown that the structural inhomogeneities observed in the studied alloy at the atomic level (clusters of atoms with a large radius) actively influence the mechanical and acoustic properties of the material.
- Based on thermal activation analysis of the process of macroscopic active plastic deformation, estimates were obtained of the density of local obstacles controlling the movement of dislocations $\sim 260 \cdot b^2$ m^2; as well as the distance between local obstacles in the slip plane $\sim 16 \cdot b \simeq 4$ nm; and the length of straight lines segments of dislocation lines located in the valleys of first kind Peierls relief ~ 10 nm. This distance turned out to be the same as the length dislocation segments, the separation of which from point defects causes the anomaly of acoustic absorption at $T_p \simeq 230$ K. This empirical estimate aligns with the experimentally observed distances between clusters of atoms with a relatively large atomic radius in [4], which induce local distortions in the crystal lattice and serve as substantial barriers to dislocations.
- Quantitative estimates have been made for the key characteristics of kinetic a dynamic of dislocations:
  1. The Einstein temperature of the material under study is $\Theta_E = 160$ K.
  2. An estimate $\sim 4 \cdot 10^{13} m^{-2}$ of the overall length of dislocation segments per unit volume was obtained within the Koiwa-Hasiguti model for the relaxation process of sound absorption at $T_p \simeq 230$ K. The obtained value is less than the value $\sim 5 \cdot 10^{15} m^{-2}$ of overall dislocation density obtained by the X-ray diffraction analysis. This aligns with the notion that a substantial fraction of dislocations are concentrated at grain boundaries, while only those segments situated within grains and oriented favourably relative to the propagation direction of sound waves can efficiently engage with the cyclic deformation of the sample.
  3. The estimate for the speed of sound $3.4 \cdot 10^3 \frac{m}{s}$, obtained in the continuum approximation of a dislocation string within the framework of the Seeger relaxation model of the sound absorption peak at $T_p^s = 190$ K is in good agreement with the direct experimental data of the works [2], [3].
  4. The empirical estimates obtained by analyzing the absorption peak $T_{ps} = 190$ K for the energy per unit length of a dislocation $\Gamma \simeq 13 \cdot 10^{-9} \frac{J}{m} \approx 2 \cdot Gb^2$ and the linear mass density $M \simeq 10^{-15} \frac{\text{kg}}{m} \approx 2 \cdot \rho b^2$ do not contradict their estimates in the continuum theory of dislocations $\Gamma \approx Gb^2$ and $M \approx \rho b^2$.

5. Through the analysis of low-temperature acoustic resonances in the studied HEA, it was determined that in it the Peierls stress $\tau_{p1} \approx 4 \cdot 10^6$ Pa for dislocations in the easy slip system is significantly less than the low-temperature values of the yield strength $\tau_2 \approx 2 \cdot 10^8$ Pa $\simeq 50 \cdot \tau_{p1}$.

Acknowledgments

The authors thank Dr. Damian Szymański for conducting $Al_{0.5}CoCrCuFeNi$ alloy elemental composition measurement.

This work was partly supported by the NRFU (Grant 2023.03/0012); Projects No. 0122U001504 and No. 0124U000272 NAS of Ukraine and internship within the framework of scientific cooperation between the National Academy of Sciences of Ukraine and the Polish Academy of Sciences.

References

[1] Y. Semerenko, V. Natsik, E.D. Tabachnikova, Y. Huang and T.G. Langdon, Mechanisms of Low-Temperature Dislocation Motion in High-Entropy $Al_{0.5}CoCrCuFeNi$ Alloy, Metals **14** (2024), 778. DOI: 10.3390/met14070778

[2] O.S. Bulatov, V.S. Klochko, A.V. Korniyets, I.V. Kolodiy, O.O. Kondratov, T.M. Tikhonovska, Low temperature elastic properties of $Al_{0.5}CoCrCuFeNi$ high-entropy alloy, Funct. Mater. **28** (2021) 492-496. DOI: 10.15407/fm28.03.492

[3] V.S. Klochko, A.V. Korniyets, I.V. Kolodiy, O.O. Kondratov, V.I. Sokolenko, V.I. Spitsyna, T.M. Tykhonovska, and N.A. Yayes, Ultrasonic Investigation of High-Entropy $Al_{0.5}CoCrCuFeNi$ Alloy at Low Temperature, Metallofiz. Noveishie Tekhnol. **45**(4) (2023) 523–535. DOI: 10.15407/mfint.45.04.0523

[4] E.J. Pickering, H.J. Stone, N.G. Jones, Fine-scale precipitation in the high-entropy alloy $Al_{0.5}CrFeCoNiCu$, Mat. Sci. Eng. **A645** (2015) 65-71. DOI: 10.1016/j.msea.2015.08.010

[5] M.O. Laktionova, O.D. Tabachnikova, Z. Tang, P.K. Liaw, Mechanical properties of the high-entropy alloy $Al_{0.5}CoCrCuFeNi$ at temperatures of 4.2–300 K, Low Temp. Phys. **39** (2013) 630-632. DOI: 10.1063/1.4813688

[6] Yu.O. Semerenko, O.D. Tabachnikova, T.M. Tikhonovska, I.V. Kolodiy, O.S. Tortika, S.E. Shumilin, and M.O. Laktionova, Temperature Dependence of the Acoustic and Mechanical Properties of Cast and Annealed High-Entropy $Al_{0.5}CoCuCrNiFe$ Alloy, Metallofiz. Noveishie Tekhnol. **37(**11) (2015) 1527-1538. (in Russian)

[7] E.D. Tabachnikova, M.A. Laktionova, Yu.A. Semerenko, S.E. Shumilin, A.V. Podolskiy, M.A. Tikhonovsky, J. Miskuf, K. Csach, Mechanical properties of $Al_{0.5}CoCrCuFeNi$ high entropy alloy in different structural states in temperature range 0.5–300 K, Low Temp. Phys. **43**(9) (2017) 1108-1118. DOI: 10.1063/1.5004457

[8] Yu.A. Semerenko and V.D. Natsik, Low temperature peak of internal friction in high entropy $Al_{0.5}CoCrCuFeNi$ alloy, Low Temp. Phys. **46** (2020) 78-86. DOI: 10.1063/10.0000367

[9] V.D. Natsik, Yu.O. Semerenko, E.D. Tabachnikova, Dislocation mechanisms of acoustic relaxation and plastic deformation of a high-entropy alloy $Al_{0.5}CoCrCuFeNi$ under moderate to deep cooling conditions: Experiment and theory (Review), Low Temp. Phys. **51** (2025) 282-299. DOI: 10.1063/10.0035810

[10] L.I. Mirkin, Handbook of X-Ray Analysis of Polycrystalline Material, Consultants Bureau, New York, 1964. 731 pp.

[11] V.D. Natsik, Yu.A. Semerenko, Dislocation mechanisms of low-temperature acoustic relaxation in iron, Low Temp. Phys. **45**(5) (2019) 551-567. DOI: 10.1063/1.5097366

[12] M. Koiwa, R.R. Hasiguti, A theory of internal friction peak due to thermal unpinning of dislocations and its application to P1 peak in copper, Acta Met. **13** (1965) 1219-1230. DOI: 10.1016/0001-6160(65)90032-5

[13] D.H Niblett, Bordoni Peak in Face-Centered Cubic Metals // In Physical Acoustics, Ed. W.P. Mason, V. III, part. A, Academic Press, New York, (1964), 428pp.

[14] A. Seeger, On the theory of the low-temperature internal friction peak observed in metals, Phyl. Mag. **1** (1956) 651-662. DOI: 10.1080/14786435608244000

[15] E. Tabachnikova, T. Hryhorova, S. Shumilin, Y. Semerenko, Yi. Huang, Terence G. Langdon, Cryo-Severe Plastic Deformation, Microstructures and Properties of Metallic Nanomaterials at Low Temperatures, Mater. Trans. **64**(8) (2023) 1806-1819. DOI: 10.2320/matertrans.MT-MF2022037